Tetrahedron Letters 69 (2021) 152972

Contents lists available at ScienceDirect

Tetrahedron Letters

journal homepage: www.elsevier.com/locate/tetlet

Regulation of aggregation-induced emission color of α-cyanostilbene luminogens through donor engineering of amino derivatives

Murat Tonga *

Department of Chemistry, University of Massachusetts, Amherst, MA 01003, United States

ARTICLE INFO

Article history:
Received 14 December 2020
Revised 23 February 2021
Accepted 26 February 2021
Available online 2 March 2021

Keywords:
Aggregation-induced emission
α-Cyanostilbene
Color-tunability
Substituent effect

ABSTRACT

In this contribution, α-cyanostilbene-based D-π-A-π-D type compounds consisting of different substituents on the amino donor group (e.g., fused, aryl/alkyl, and dialkyl) were designed, synthesized and their aggregation-induced emission was investigated thoroughly. The incorporation of these substituents furnished AIE features with tunable emission colors ranging from green-to-yellow-to-red. The compounds all showed a weak emission in THF; however, they showed an enhanced emission upon addition of water by forming emissive aggregates, which may arise from the restriction of twisted intramolecular charge transfer and *E*/*Z* isomerization. The DFT calculations revealed that the luminogens adopted distinctive conformations including a highly twisted one and a relatively coplanar one with the variation in the amino substituents.

Organic π-conjugated compounds have been extensively investigated for optical and electronic applications [1]. The majority of these compounds are very emissive in dilute solution but tend to become weakly emissive or non-emissive at the solid states due to the formations of unfavorable species such as excimers as a result of strong π-π interactions in the aggregate [2]. This is known as aggregation-caused quenching (ACQ) which has significantly restricted their applications since they are typically employed in aggregated or solid states [3]. However, the luminescent materials require having a high luminescence efficiency to work primarily at the solid-state. In 2001, this key challenge has been attempted by Tang and coworkers with the proposition of a new and an opposite phenomenon, so-called aggregation-induced emission (AIE) [4]. In this concept, AIE luminogens demonstrate weak emission in solution, but a strong emission in the aggregate or solid-state. The accepted mechanism is the restriction of intramolecular motions (RIM) which can be obtained by planarization in the configuration, formation of *J*-aggregate, *E*/*Z* isomerization, twisted intramolecular charge transfer (TICT), and excited-state intramolecular proton transfer (ESIPT) [5]. Since then, AIE luminogens have become of great advanced materials in particular applications including organic light emitting devices (OLEDs), sensing, and imaging [6].

In general, the AIE compounds can be categorized by their structural aspects: hydrocarbon, heterocyclic, α-cyanostilbene, hydrogen-bonding, polymeric, organometallic, and miscellaneous luminogens [7]. Among them, α-cyanostilbene has been intensively studied as a functional moiety in the AIE compounds due to its simple structure and high polarizability [8]. Despite the small size of nitrile in the α-cyanostilbene structure, it can still induce steric impacts in the surrounding groups which cause a twisted conformation. Also, its electron-withdrawing feature enables to design donor-acceptor type π-conjugated compounds showing desired optical features. Besides, intramolecular charge transfer (ICT) commonly observed in the donor–acceptor type π-conjugated systems plays a significant role in the photophysical behaviors of AIE luminogens, particularly the emission color [9].

The AIE luminogens with tunable colors (emissions) have found tremendous attention in optoelectronic devices and biotechnology [10]. The molecular packing of the luminogens at the solid-state is significantly affected by the substituents on the luminogens which has no direct electronic contribution to π-conjugated emissive core. Particularly, side-chain substituents have demonstrated a dramatic impact on the emission properties such as color and quantum yield. For instance, Imoto et al showed the effect of the chain length, hydroxyl group, and branching structure on the AIE properties of *N*-alkyl arylaminomaleimide dyes [11]. Dong et al reported the effects of side chains on AIE properties of water-soluble TPE derivatives [12]. In another study, Zhang et al investigated the chain length-dependent behavior of 9,10-bis[(N-alkylphenothiazin-3-yl)vinyl]anthracene compounds [13]. Herein, in the present paper, novel AIE luminogens with D-π-A-π-D configuration were developed using amino derivatives as a donor unit and cyano as an acceptor unit. The emission properties of the luminogens can

* Address: Polnox Corporation, 225 Stedman St Suite 23, Lowell, MA 01851, United States.

https://doi.org/10.1016/j.tetlet.2021.152972
0040-4039/

be rationally tuned at the aggregate state emitting from green-to-yellow-to-red. The introduction of amino derivatives with various substituents into the π-conjugated α-cyanostilbene configuration results in not only a highly twisted conformation but also a planar one, which generated distinctive AIE properties.

The synthetic routes for AIE luminogens **CZ**, **DPA** and **DMA** are shown in Scheme 1. Synthetic details are given in the Supporting Information. The Knoevenagel condensation reaction between a terminal aldehyde on the donor moieties and an activated methylene group on the acceptor (1,4-phenylenediacetonitrile) (**6**) gave all D-π-A-π-D type luminogens in the presence of a base catalyst potassium-*t*-butoxide. The synthetic approach for the donor compounds starts with the alkylation of amino donors. The intermediate compounds **1** and **3** which are the alkylation of carbazole and diphenylamine, respectively, were prepared according to procedures described previously [14]. Vilsmeier-Haack formylation readily yielded the intermediates **2** and **4** consisting of a terminal aldehyde group on the alkylated amino donor compounds. Commercially available donor 4-(dimethylamino)benzaldehyde (**5**) was used as-is. The synthesis of **DMA** has been previously reported [15]. Notably, all luminogens demonstrated good solubility in common organic solvents such as dichloromethane, chloroform, THF, acetone, and acetonitrile. The resulting AIE luminogens were thoroughly characterized by H^1 NMR and high-resolution mass spectrometry.

The optical properties (the UV–vis absorption and photoluminescence (PL) spectra) of the AIE luminogens **CZ**, **DMA** and **DPA** were investigated in THF solution. The UV–vis absorption and PL spectra of the luminogens are shown in Fig. 1 and the corresponding photophysical data are presented in Table 1. The solution absorption spectroscopy of the luminogens endows the understanding of their excited state behavior, mainly ICT character which is a common process noted in the donor–acceptor compounds. Generally, the combination of electron-donating groups, including alkyldiphenylamine or carbazole, and electron-withdrawing groups such as cyano leads to an ICT process in the luminogens. The ICT absorptions of the luminogens **DPA** and **DMA** are similar due to nearly identical electron-donating strengths. As an example, the solvatochromic behavior of the luminogen **DMA** was shown in various solvents (Fig. S3). The maximum absorption peak of these luminogens is located at ~428 nm, while it is at 409 nm for the luminogen **CZ**. A redshift by about 20 nm suggests that the alkyldiphenylamine and dimethylamine groups are a stronger electron-donor than the carbazole group

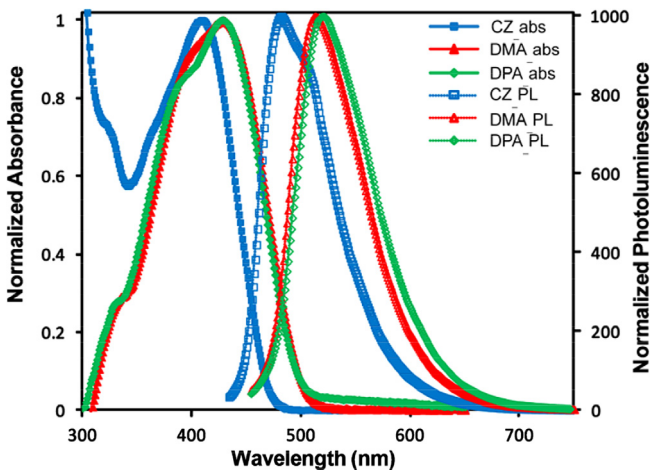

Fig. 1. Normalized absorption (a) and normalized photoluminescence spectra (b) of the luminogens in THF.

[16]. The luminogens absorb strongly through the blue region with band onsets at 500–525 nm.

The luminogens showed weak photoluminescence at the solution state. The normalized PL spectra are shown in Fig. 1b. A similar trend was observed in the PL spectra, as was noted for their absorbance spectra. Red-shifting maxima of from 482 to 520 nm were observed with increasing electron-donating ability of the donor segments, **DPA** has the largest shift (91 nm) and **CZ** has the lowest shift (73 nm). Related Stokes shifts are also shown in Table 1. The large Stokes shifts suggest for large dipole moment change at the excited state.

Molar extinction coefficients of the luminogens are presented in Table 1. All the luminogens exhibited quite high molar extinction coefficients ranging from 57,400 M^{-1} cm^{-1} to 77,300 M^{-1} cm^{-1} at the maximum absorption wavelength (λ_{max}) in THF. The luminogen **DMA** showing the highest extinction coefficient might be due to its coplanar geometry compared to **CZ** and **DPA**.

The luminogens are soluble in THF, but insoluble in water. To investigate aggregation-induced emission aspects of the luminogens, photoluminescence spectra were evaluated at 5 μM of the luminogens in THF with different water fractions (f_w) changing from 10% to 90%. With the addition of the high fraction of water, well-dispersed state in THF was altered to the aggregate state, which ultimately affects the emission properties. Fig. 2

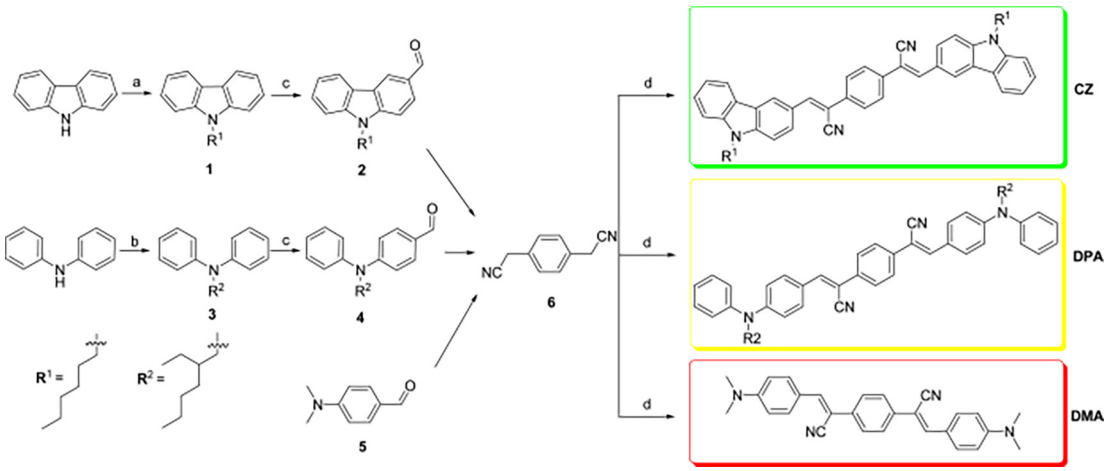

Scheme 1. Synthetic route to the luminogens CZ, DPA and DMA. (a) 1-bromohexane, 18-crown-6, KOH, toluene, 110 °C, 20 h, 96%. (b) 2-ethylhexylbromide, NaOH, DMSO, 110 °C, 24 h, 80%. (c) $POCl_3$, DMF, 100 °C, 15 h, 34% (2) and 7% (4). (d) *t*-BuOK, ethanol, reflux, 16 h, 74% (CZ), 67% (DPA), 90% (DMA).

Table 1
Photophysical data of the luminogens.

	Abs_{max} (nm)	PL_{max} (nm)	Abs_{onset} (nm)	ϵ ($M^{-1}cm^{-1}$)	Stokes Shift (cm^{-1})	E_g^{opt} (eV)[a]
CZ	409	482	502	67,600	3703	2.47
DMA	428	513	505	77,300	3871	2.46
DPA	429	520	525	57,400	4079	2.36

[a] E_g^{opt}: optical band gap, estimated from UV–vis absorption edge.

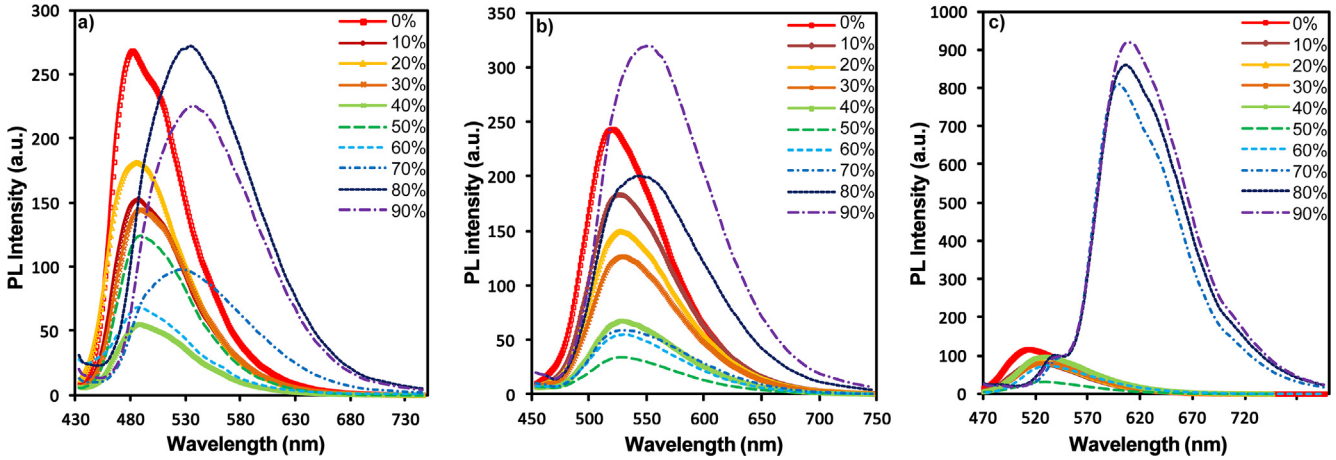

Fig. 2. Photoluminescence spectra of the luminogens in THF-water mixtures: (a) CZ, (b) DPA, and (c) DMA.

demonstrates the PL change upon the addition of water to the THF solution.

CZ has a D-π-A-π-D structure and rotator alkyl segments which allow demonstrating typical AIE behaviors. The PL intensity of **CZ** showed a continuous decrease until the f_w reached 70% with some irregularities at the water fractions of 20% and 50% (Fig. 2a). This weakened PL intensity can be ascribed to a change in the solvent polarity. Upon addition of water, the molecules can form weakly emitting crystalline aggregates, intensely emitting amorphous aggregates, or both [17]. In the crystalline state, the molecules pack in a well-ordered structures, but they can easily undergo strong intermolecular π-π interactions that quench or weaken the emission intensity.

However, in the amorphous state, the randomly ordered molecules due to the weak intermolecular interactions can activate the RIM, thereby improving the emission intensity. The emission of **CZ** starts to intensify after adding f_w = 70% by reaching the intensity of the pure THF solution. A possible explanation for this behavior could be the formation of amorphous aggregates which typically increase the emission.

A similar AIE and twisted intramolecular charge transfer (TICT) phenomenon were also observed for the luminogen **DPA** due to the strong D-A impact and intramolecular rotations in its molecular structure. To investigate the AIE features of the **DPA**, different water fractions were added to the pure THF solutions. Fig. 2b demonstrates that the PL intensity decreases gradually with the f_w < 50%, and starts to increase gradually at the f_w = 50–70%. Then, it intensifies significantly when the f_w > 80%, with emitting yellow light (λ_{em} = 551 nm) under illumination with a 365 nm UV lamp (Fig. 3b-inset). In the solutions with dilute water fractions, the intramolecular motions such as phenyl and alkyl rotations can switch the excited-state energy to non-radiative, causing a decrease in the emission by possibly generating crystalline aggregates. At high water fractions, the aggregates could rearrange into a less ordered fashion to form amorphous aggregates, which usually enhance the PL intensity [18]. In addition, at higher f_w, the twisted nature of the alkylated diphenylamine moiety also limits intermolecular π-π stacking, which generally diminishes the aggregate emission and therefore rendering the compound **DPA** to emit intensely. The change in the PL peak intensity (I/I_0 ratio) was plotted in Fig. 3b. When the f_w = 90%, the peak intensity rose by about 13-times in comparison with the f_w = 50%, which is the most quenched state and it was roughly enhanced by 1.2-times compared to in the pure THF solution. AIE property occurred with redshifts of 5–13 nm for the added f_w = 10–70%, it was red-shifted by 24–31 nm when the f_w > 70%. These redshifts are lower than that of the luminogens **CZ** and **DMA**, which is possibly due to **DPA** possessing many rotator groups [19].

The pure THF solution of **DMA** is less emissive in comparison with those of **CZ** and **DPA** due to the restricted intramolecular motions of short alkyl chains which deplete excited state energy by non-radiative decay (Fig. 2c). Similarly, when the f_w < 60% in the mixed solution, the emission is more quenched, which can be attributed to the formation of the crystalline aggregates upon the variation in the solvent polarity. The raised polarity of the solvent progressively stabilizes the TICT process and leads to a decrease in the emission [20]. The change in the PL intensity (I/I_0 ratio) with the change in f_w was also investigated (Fig. 3c). Once the f_w reached 70% or more, a drastic improvement was observed in the red emission which is 10-times higher than that in pure THF. In addition, the emission intensity was improved up to ~50 times compared to the most quenched state which was prepared with the added f_w = 50%. It can be explained that the formation of the aggregates limits the rotational motions of the -NMe_2 group, and thereby enhancing the emission. Hence, **DMA** exhibits typical AIE behaviors. And also, this type of photophysical behavior is very common in the structures having strong donor–acceptor interaction [21]. The improvement in the PL intensity was also accompanied by 8–20 nm of redshifts in the PL peak for the added f_w up to 60%, then 85–95 nm redshifts for the added f_w > 60%, which is typical AIE characteristics. Thus, the aggregates of **DMA** that were created with a higher amount of water fraction showed red emission

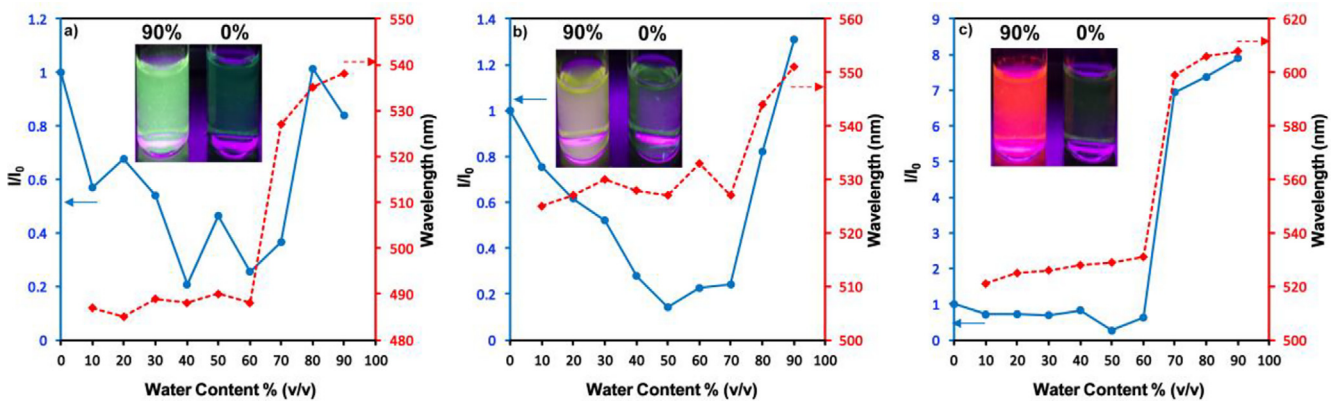

Fig. 3. The changes in the PL intensity and λ_{max} in THF-water mixtures with f_w = 10–90%: (a) CZ, (b) DPA and (c) DMA. Inset: fluorescent images of the luminogens in THF–water mixtures at the f_w = 90% and f_w = 0% under illumination with a 365 nm UV lamp.

peaked at 608 nm under illumination with a 365 nm UV lamp (Fig. 3c-inset). Notably, these luminogens demonstrated color-tunable properties from green-to-yellow-to-red by simply controlling the water fractions in the mixed solvent system.

The CIE 1931 coordinates of the luminogens are shown in the chromaticity diagram in Fig. S4. Specifically, three types of emissions were observed with the change in water content in the aggregate state. For instance, the luminogen **CZ** displayed a cyan emission at the f_w > 40%, a green emission at the f_w = 40–60%, a cyan emission at the f_w = 70%, which is anomalous shifting to lower wavelengths, and a green emission at the f_w > 70% (Fig. 4S-a). **DPA** showed a yellowish-green emission at the f_w = 10–60%, a yellow-green emission at the f_w = 60–80%, and a yellow emission at the f_w = 90% (Fig. 4S-b). **DMA** showed a quite different color palette than **CZ** and **DPA**: a yellowish-green emission at the f_w = 10–50%, a yellow-green emission at the f_w = 60%, and a red emission at the f_w = 70–90% (Fig. 4S-c).

To gain insight into the relationship between the structures and AIE properties of the luminogens, optimized geometry, and molecular frontier orbitals were studied by density functional theory (DFT) using the Spartan 04 program at the B3LYP/6-31G** level (Fig. 4) when the crystal structures are not available. The luminogens all demonstrated similar highest occupied molecular orbital (HOMO) electron distributions which are mostly delocalized throughout the entire π-conjugated backbone. Cyano, alkyls, and peripheral phenyl groups have no contributions to the HOMO levels. The lowest unoccupied molecular orbital (LUMO) electron distributions in all luminogens were similar to one another, were mainly located in the central region including cyano acceptor groups, vinylenes, and the central phenylene. Clearly, such an electronic distribution reveals intense ICT attributes in the D-π-A-π-D type luminogens, which may induce quenched or diminished PL in moderately polar solvents like THF. This behavior is often observed to decay from the excited state to the ground state via non-radiative channels [22]. Also, these findings are consistent with the spectroscopic results. In the absence of crystal structures, optimized geometries could be beneficial to understand the structural features. Their optimized structures are given in Fig. 4. The DFT calculations revealed that the overall planarity of the luminogens increases in the order of **CZ > DPA > DMA**.

The dihedral angles between the electron-withdrawing cyano group, the conjugated phenylene group on the electron-donating amino group and the central phenylene building block were investigated. Particularly, dihedral angle α is defined between the electron-withdrawing cyano moiety and the central phenylene; β is defined between the electron-withdrawing cyano moiety and the phenylene on the electron-donating amino group which participates π-conjugation in the backbone; γ is defined between the central phenylene and the phenylene on the electron-donating amino group which participates π-conjugation in the main plane. Table 2 shows the calculated dihedral angles, HOMO, LUMO, and electronic band gap for all the luminogens. Using the DFT computational analysis, electronic band gaps were also calculated in the range of 2.96–3.15 eV, which are consistent with spectroscopic results. In general, cyano electron-accepting groups are pushed out of the central backbone due to steric hindrance with neighboring phenyl rings in these luminogens. In the solution state, the excited state energy can be deactivated through non-radiative transitions such as vibrational and rotational motions of the substituent moieties on the vinylic double bond, thereby resulting in minimal emission.

As illustrated in Fig. 4, **CZ** and **DPA** adopt highly twisted propeller-like conformations. Dihedral angles for **CZ** were found as α = 19.9°, β = 10.5° and γ = 43.8°. The calculated dihedral angles were higher for **DPA** due to rotary N,N-alkyldiphenyl amino groups: α = 21.3°, β = 13.6°, and γ = 49°. Overall, **CZ** shows better planarity than **DPA** due to the extended conjugation. In the aggregate state, such torsional angles due to free rotations are extensively limited in **CZ** and **DPA**. Thus, the formation of detrimental species is suppressed by inducing intense emission. **DMA** exhibited a highly planar conformation compared to **CZ** and **DPA**. The presence of small dimethylamino groups increased the rigidity of π-conjugated backbone by forming a less twisted geometry relative to the luminogens **CZ** and **DPA**. Dihedral angles for **DMA** were calculated as α = 19.9°, β = 3.9° and γ = 36.2°. Showing AIE activity with such a structure is an atypical result for **DMA**. It could be explained by the photoisomerization of the vinyl double bond via an *E*/*Z* conversion upon excitation. This transformation in the excited state depletes the energy of the excited state through non-radiative pathways. However, such a conversion in the excited state is impeded or weakened in the aggregated state to allow the compounds to display an intense emission [23]. The *E*/*Z* reorganization is presumably challenging for **CZ** and **DPA** due to the steric hindrance of large alkyl groups which could prevent intermolecular stacking at the excited state. Additional experiments would be necessary to explore this further. Moreover, it can be inferred that a large twisted conformation gave green and yellow emission while a small one gave a red emission.

This work shows a practical synthetic methodology for modulating emission color by varying the functionalities on the donor moieties. Connecting amino derivatives to α-cyanostilbene through π-conjugation in the D-π-A-π-D structures yielded the AIE luminogens with color-tunable emission ranging from green-to-yellow-to-red. Specifically, the emission was readily tuned by

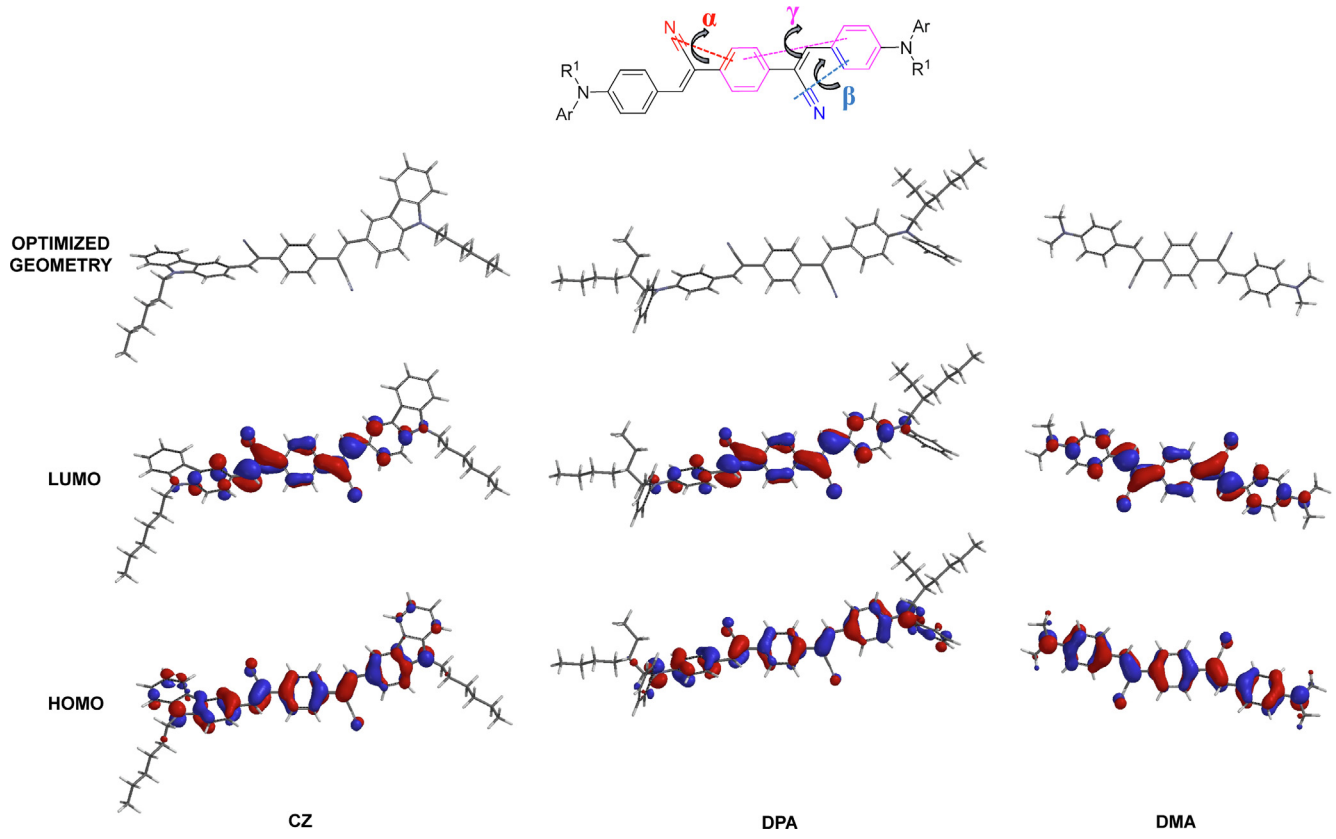

Fig. 4. Description of dihedral angles, the optimized geometry, and frontier molecular orbitals of the luminogens.

Table 2
Computational data of the luminogens.

	α (°)	β (°)	γ (°)	E_{HOMO} (eV)	E_{LUMO} (eV)	E_g^{DFT} (eV)
CZ	19.9	10.5	43.8	−5.18	−2.03	3.15
DMA	19.9	3.9	36.2	−4.9	−1.88	3.02
DPA	21.3	13.6	49	−4.7	−2.01	2.96

changing the π-skeleton (*e.g.*, fused ring) and the substituents (*e.g.*, *N, N*-alkyl/diphenyl and *N*,*N*-dimethyl) on the amino donor segments. The employment of the alkyl chains in **CZ** and **DPA** resulted in a twisted conformation that allowed the molecules to show AIE aspects in the aggregate state. Despite the high planarity observed in **DMA** in comparison to **CZ** and **DPA**, it displayed an AIE property that may stem from an *E*/*Z* transformation upon excitation. The DFT results also revealed that the degree of twisting plays a big role in the emission colors of the aggregate state: a large twisted orientation resulted in green and yellow emission as in the case of **CZ** and **DPA** while a small one in **DMA** gave a red emission. Therefore, this study would render luminescent materials to produce tunable AIE features that could open a versatile strategy for the development of optoelectronic applications.

Declaration of Competing Interest

The authors declare that they have no known competing financial interests or personal relationships that could have appeared to influence the work reported in this paper.

Acknowledgements

This work was supported by the Defense Threat Reduction Agency via Department of the Army through contracts W911QY-12-2-007 and W911NF-14-2-0002 from the US Army Natick Soldier Research, Development and Engineering Center (NSRDEC). Any opinions, findings, and conclusions or recommendations expressed in this material are those of the authors and do not necessarily reflect the views of the NSRDEC. The author gratefully thanks Emeritus Prof. P.M. Lahti of University of Massachusetts for providing resources for this self-guided research project.

Appendix A. Supplementary data

Supplementary data to this article can be found online at https://doi.org/10.1016/j.tetlet.2021.152972.

References

[1] a) M. Yu, R. Huang, J. Guo, Z. Zhao, B.Z. Tang, PhotoniX 1 (2020) 11–44;
b) Y. Chen, J.W.Y. Lam, R.T.K. Kwok, B. Liu, B.Z. Tang, Mater. Horiz. 6 (2019) 428–434.
[2] a) F. Mancin, P. Scrimin, P. Tecilla, U. Tonellato, Coord. Chem. Rev. 253 (2009) 2150–2165;
b) S.W. Thomas, G.D. Joly, T.M. Swager, Chem. Rev. 107 (2007) 1339–1386;
c) H.J. Tracy, J.L. Mullin, W.T. Klooster, J.A. Martin, J. Haug, S. Wallace, I. Rudloe, K. Watts, Inorg. Chem. 44 (2005) 2003–2011.
[3] a) R.H. Friend, R.W. Gymer, A.B. Holmes, J.H. Burroughes, R.N. Marks, C. Taliani, D.D.C. Bradley, D.A. Dos Santos, J.L. Bredas, M. Logdlund, W.R. Salaneck, Nature 397 (1999) 121–128;
b) S.A. Jenekhe, J.A. Osaheni, Science 265 (1994) 765–768.

[4] J. Luo, Z. Xie, J.W.Y. Lam, L. Cheng, H. Chen, C. Qiu, H.S. Kwok, X. Zhan, Y. Liu, D. Zhu, B.Z. Tang, Chem. Commun. 18 (2001) 1740–1741.
[5] J. Mei, Y. Hong, J.W.Y. Lam, A. Qin, Y. Tang, B.Z. Tang, Adv. Mater. 26 (2014) 5429–5479.
[6] a) J. Chan, S.C. Dodani, C.J. Chang, Nat. Chem. 4 (2012) 973–984;
b) T. Ueno, T. Nagano, Nat. Methods 8 (2011) 642–645;
c) Y. Chen, X. Min, X. Zhang, F. Zhang, S. Lu, L.-P. Xu, X. Lou, F. Xia, X. Zhang, S. Wang, Biosens. Bioelectron. 111 (2018) 124–130.
[7] J. Mei, N.L.C. Leung, R.T.K. Kwok, J.W.Y. Lam, B.Z. Tang, Chem. Rev. 115 (2015) 11718–11940.
[8] E.R. Jimenez, H.J. Rodríguez, Mater. Sci. 55 (2020) 1366–1387.
[9] a) H. Lu, Y. Zheng, X. Zhao, L. Wang, S. Ma, X. Han, B. Xu, W. Tian, H. Gao, Angew. Chem. Int. Ed. 55 (2016) 155–159;
b) S.-Y. Chen, Y.-W. Chiu, G.S. Liou, Nanoscale 11 (2019) 8597–8603;
c) B. Wang, Y. Wang, J. Hua, Y. Jiang, J. Huang, S. Qian, H. Tian, Chem. - Eur. J. 17 (2011) 2647–2655;
d) H. Tian, D. Li, X. Tang, Y. Zhang, Z. Yang, J. Qian, Y.Q. Dong, M. Han, Mater. Chem. Front. 4 (2020) 1634–1642.
[10] a) X. Peng, F. Song, E. Lu, Y. Wang, W. Zhou, J. Fan, Y. Gao, J. Am. Chem. Soc. 127 (2005) 4170–4171;
b) A. Zaheer, R.E. Lenkinskl, A. Mahmood, A.G. Jones, L.C. Cantley, J.V. Frangioni, Nat. Biotechnol. 19 (2001) 1148–1154;
c) C. Weder, J. Mater. Chem. 21 (2011) 8235–8236;
d) M. Wang, G. Zhang, D. Zhu, B.Z. Tang, J. Mater. Chem. 20 (2010) 1858–1867;
e) H. Ito, T. Saito, N. Oshima, N. Kitamura, S. Ishizaka, Y. Hinatsu, M. Wakeshima, M. Kato, K. Tsuge, M. Sawamura, J. Am. Chem. Soc. 130 (2008) 10044–10045.
[11] H. Imoto, K. Nohmi, K. Kizaki, S. Watase, K. Matsukawa, S. Yamamoto, M. Mitsuishic, K. Naka, RSC Adv. 5 (2015) 94344–94350.
[12] Y. Dong, W. Wang, C. Zhong, J. Shi, B. Tong, X. Feng, J. Zhi, Y. Dong, Tetrahedron Lett. 55 (2014) 1496–1500.
[13] X. Zhang, Z. Mab, Y. Yang, X. Zhang, Z. Chi, S. Liu, J. Xu, X. Jia, Y. Wei, Tetrahedron 70 (2014) 924–929.
[14] a) I. Kaya, S. Koyuncu, J. Appl. Polym. Sci. 113 (2009) 1975–1985;
b) S. Ramkumar, S. Anandan, Dyes Pigments 97 (2013) 397–404.
[15] a) S.J.K. Pond, M. Rumi, M.D. Levin, T.C. Parker, D. Beljonne, M.W. Day, J.-L. Brédas, S.R. Marder, J.W. Perry, J. Phys. Chem. A 106 (2002) 11470–11480;
b) J.S. Ramírez-Pradilla, C. Blanco-Tirado, M.Y. Combariza, ACS Appl. Mater. Interfaces 11 (2019) 10975–10987.
[16] a) W. Huang, F. Tang, B. Li, J. Sua, H. Tian, J. Mater. Chem. C 2 (2014) 1141–1148;
b) W. Huang, H. Zhou, B. Li, J. Su, RSC Adv. 3 (2013) 3038–3045.
[17] a) S. Kim, Q.D. Zheng, G.S. He, D.J. Bharali, H.E. Pudavar, A. Baev, P.N. Prasad, Adv. Funct. Mater. 16 (2006) 2317–2323;
b) Y.Q. Dong, J.W.Y. Lam, A.J. Qin, J.X. Sun, J.Z. Liu, Z. Lin, Z.Z. Sun, H.H.Y. Sung, I.D. Williams, H.S. Kwok, B.Z. Tang, Chem. Commun. (2007) 3255–3257;
c) Z.Y. Zhang, B. Xu, J.H. Su, L.P. Shen, Y.S. Xie, H. Tian, Angew. Chem., Int. Ed. 50 (2011) 11654–11657.
[18] Y.N. Hong, J.W.Y. Lam, B.Z. Tang, Chem. Commun. 29 (2009) 4332–4353.
[19] X. Zhao, P. Xue, K. Wang, P. Chen, P. Zhang, R. Lu, New J. Chem. 38 (2014) 1045–1051.
[20] Y. Liu, Y. Zhang, X. Wu, Q. Lan, C. Chen, S. Liu, Z. Chi, L. Jiang, X. Chen, J. Xu, J. Mater. Chem. C 2 (2014) 1068–1075.
[21] P. Mazumdar, D. Das, G.P. Sahoo, G. Salgado-Morán, A. Misra, Phys. Chem. Chem. Phys. 16 (2014) 6283–6293.
[22] Z. Peng, Y. Ji, Z. Huang, B. Tong, J. Shi, Y. Dong, Mater. Chem. Front. 2 (2018) 1175–1183.
[23] a) J.-S. Ni, H. Liu, J. Liu, M. Jiang, Z. Zhao, Y. Chen, R.T.K. Kwok, J.W.Y. Lam, Q. Peng, B.Z. Tang, Mater. Chem. Front. 2 (2018) 1498–1507;
b) L. Yang, P. Ye, W. Li, W. Zhang, Q. Guan, C. Ye, T. Dong, X. Wu, W. Zhao, X. Gu, Q. Peng, B.Z. Tang, H. Huang, Adv. Opt. Mater. 6 (2018) 1701394.